

Self-consistent orbital evolution of a particle around a Schwarzschild black hole

Peter Diener,^{1,2} Ian Vega,³ Barry Wardell,^{4,5} and Steven Detweiler⁶

¹Center for Computation & Technology, Louisiana State University, Baton Rouge, LA 70803, U.S.A.

²Department of Physics & Astronomy, Louisiana State University, Baton Rouge, LA 70803, U.S.A.

³Department of Physics, University of Guelph, Guelph, Ontario, N1G 2W1, Canada

⁴Max-Planck-Institut für Gravitationsphysik, Albert-Einstein-Institut, 14476 Potsdam, Germany

⁵School of Mathematical Sciences and Complex & Adaptive Systems Laboratory,
University College Dublin, Belfield, Dublin 4 Ireland

⁶Institute for Fundamental Theory, Department of Physics,
University of Florida, Gainesville, FL 32611-8440, U.S.A.

The motion of a charged particle is influenced by the self-force arising from the particle's interaction with its own field. In a curved spacetime, this self-force depends on the entire past history of the particle and is difficult to evaluate. As a result, all existing self-force evaluations in curved spacetime are for particles moving along a fixed trajectory. Here, for the first time, we overcome this long-standing limitation and present fully self-consistent orbits and waveforms of a scalar charged particle around a Schwarzschild black hole.

PACS numbers: 04.20.-q, 04.25.-g, 04.70.Bw, 04.25.D-, 04.25.dg, 04.25.Nx, 97.60.Lf

In spite of the impressive progress made towards tackling the two-body problem in general relativity [1], there remains an important regime that appears to be intractable by the methods of numerical relativity. When the system consists of a massive black hole ($M \gtrsim 10^6 M_\odot$) and a stellar mass companion ($m \sim 10 M_\odot$), the disparity of length scales characterizing this black hole binary proves to be a significant roadblock for existing numerical relativity codes.

The dynamics of such a binary is intuitively simple: A slow adiabatic inspiral of the small black hole towards the bigger one is followed by an abrupt plunge towards the latter's event horizon. However, for the purposes of gravitational wave astronomy, this qualitative picture is inadequate. The ubiquity of supermassive black holes residing in galactic centers has made extreme-mass-ratio inspirals (EMRIs) one of the more prominent predicted sources of low-frequency gravitational waves for future space-based missions [2]. The science we will gain from these sources — among them precision tests of general relativity in the strong-field regime [3] and a better census of black hole populations [2, 4] — rests on our ability to model them to an exquisite degree of accuracy. Specifically, we wish to be able to track the phase of their gravitational waveforms throughout the long inspiral.

In the self-force approach to modeling EMRIs, one ignores the internal dynamics of the smaller black hole and treats it as a massive particle that distorts the spacetime geometry of the bigger partner. An EMRI is then equivalent to a charged particle moving in a black hole spacetime. But for this approach to suffice, the motion of the particle and the resulting waveform need to incorporate self-force effects arising from the interaction of the particle with its own field.

Evaluating the self-force is a difficult, though by now well understood, process [5, 6]. In a curved spacetime, the field generated by a particle at one time backscatters off the curvature and interacts with the particle at a much later time. Consequently, the self-force at any given instant depends on the particle's entire past history [7]. This restricts the usefulness of purely analytical self-force calculations mainly to astrophysically uninteresting cases [8]. On the other hand, the distributional nature of the point source makes numerical

evaluation of the self-force technically involved. The retarded field diverges at the location of the particle, thus requiring a delicate regularization to extract the finite self-force [6]. A practical scheme for dealing with this difficulty exists; this is the spherical-harmonic-based mode-sum method of Barack and Ori [9]. This method has been tremendously successful for self-force calculations based on a specified particle orbit [10–13]. However, it has not yet been applied to compute the self-force based on an evolved orbit.

A problem that has resisted solution for a long time is the computation of *self-consistently* self-forced orbits and their corresponding waveforms. These are orbits that reflect the true motion of the particle as it is driven by its actual local field. In principle, these self-consistent orbits can be obtained only by simultaneously solving the equations governing the coupled dynamics of the particle and its field.

This notion of self-consistency is what we wish to highlight, particularly because a recent manuscript [14] also reports on self-forced orbits, though not of the sort we present here. In that work, the applied self-force at some instant is not what arises from the actual field at that same instant. Instead, this applied self-force is what would have resulted if the particle were moving for all eternity along the geodesic that only instantaneously matches the true orbit; it is the “geodesic” self-force and not the self-consistent self-force. It is quite likely that the error incurred by this assumption becomes negligible in the adiabatic limit, for which the particle stays close to the instantaneous geodesic for sufficiently long times. We emphasize, however, that this is presently just an expectation rather than a demonstrated fact. Rigorously assessing its validity requires comparison with fully self-consistent orbits.

In this *Letter*, we present for the first time such fully self-consistent orbits and waveforms, albeit for a radiating scalar charge in the Schwarzschild spacetime. An example is displayed in Figs. 1 and 2.

Effective source approach:— A novel strategy for self-force calculations was proposed [15] to address the difficulties arising from a δ -function source. Its core idea is to refrain from solving the retarded field altogether and to work instead with the equation for a field Φ^R from which the self-force is readily

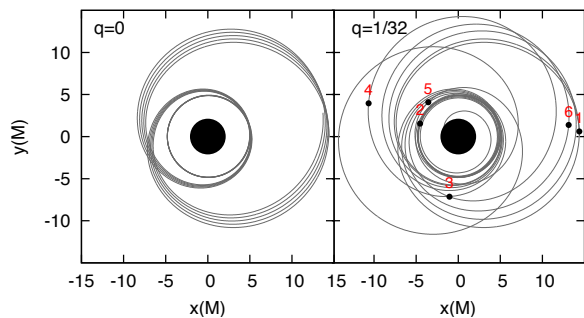


FIG. 1. (Color online) Orbits for neutral and charged particles starting at $p = 7.2$, $e = 0.5$. The orbital evolution is started close to apastron (at $t = t_1$) and the dots represent events at times $t_1 = 400M$, $t_2 = 600M$, $t_3 = 1100M$, $t_4 = 1300M$, $t_5 = 1800M$ and $t_6 = 2043.8M$, the instant of plunge. The coordinates $\{x, y\} = \{r \cos \phi, r \sin \phi\}$ are Cartesian coordinates in the equatorial plane.

computed: $f_\alpha \equiv \bar{q} \nabla_\alpha \Phi^R$, where \bar{q} is the charge of the particle. The *effective* source $S(x^\alpha | z^\alpha(\tau), u^\alpha(\tau))$ for Φ^R is C^0 (continuous but not differentiable) by construction at the location of the particle, in contrast to the traditional δ -function source for point particles. Like the δ -function source, S depends on the particle's position $z^\alpha(\tau)$ and four-velocity $u^\alpha(\tau)$. (A similar approach is independently being pursued in Ref. [16], the main difference there being that it uses a mode decomposition in the azimuthal direction). The strategy rests on Detweiler and Whiting's insight [17] that there exists a smooth solution to the vacuum field equation to which the self-force can be fully attributed. This solution is just the difference between the retarded field Φ^{ret} and a locally constructible singular field Φ^S which is the curved spacetime analogue of a ‘‘Coulomb’’ field that does not contribute to the self-force. Our approximation to the regular field Φ^R differs from the smooth Detweiler-Whiting solution by terms that scale as $O(\rho^3)$ as $\rho \rightarrow 0$, where ρ is some appropriate measure of distance from the particle. It is thus only a C^2 approximation to the Detweiler-Whiting vacuum solution, but it nevertheless gives the same self-force. The limited differentiability of Φ^R comes from the inability to write down an explicit expression for the full singular field from which the effective source is constructed. Generally, only approximate expressions for Φ^S are known [11]. The construction of our expression for S is described in detail elsewhere [18].

With the effective source at hand, one needs to solve the following system of equations:

$$\square \Phi^R = S(x | z(\tau), u(\tau)) \quad (1)$$

$$\frac{Du^\alpha}{d\tau} = a^\alpha = \frac{\bar{q}}{m(\tau)} (g^{\alpha\beta} + u^\alpha u^\beta) \nabla_\beta \Phi^R \quad (2)$$

$$\frac{dm}{d\tau} = -\bar{q} u^\beta \nabla_\beta \Phi^R, \quad (3)$$

where $m(\tau)$ is the rest mass of the particle. Quinn [19] found that the rest mass is dynamically modified by the component of the self-force tangent to the four-velocity; this is reflected in Eq. (3). In all our simulations, we take the initial rest mass $m(\tau = 0)$ to be M . Because of the way S is constructed, Φ^R is equal to the retarded field in the wavezone. Thus, by solv-

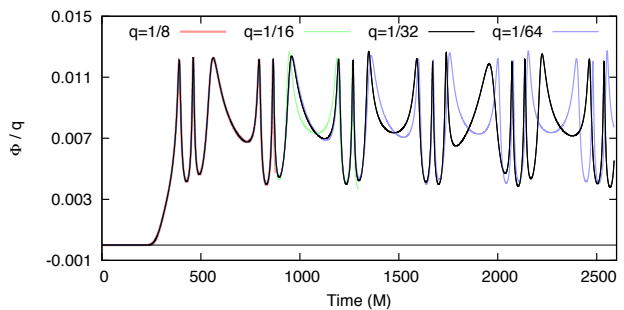


FIG. 2. (Color online) Waveforms from self-consistently evolved orbits as detected by an observer located in the orbital plane at \mathcal{I}^+ .

ing the system of equations above, one obtains not only self-forced orbits but their corresponding waveforms as well (see Figs. 1 and 2).

We recently developed code that solves Eq. (1) for a specified geodesic in the Schwarzschild spacetime [20]. Comparing with Ref. [12] we find that our main source of error is high frequency noise due to nonsmoothness of the effective source in the vicinity of the worldline. Most of the time the amplitude of this noise is small but it reaches a peak of about 2% of the value of the self-force at periaapsis.

We then evolve self-consistent orbits by supplementing the scalar field evolution with an orbit integrator. Together they allow solving Eqs. (1), (2) and (3) simultaneously. We deal with the particle motion in two ways: first by straightforward integration of Eq. (2) and second by adopting the osculating orbits framework described in Ref. [21]. The first method is more general in that it allows us to track the motion of the particle all the way to the event horizon. On the other hand, the second method, which works only for bound orbits, allows us to more readily identify aspects of the evolution that would be completely missed by methods relying on flux-averaging and balance arguments. For the regimes in which both methods are valid, we find the resulting orbits in excellent agreement.

Self-consistent orbits:– The spherical symmetry of the Schwarzschild geometry implies that test-particle orbits may always be described by motion in the $\theta = \pi/2$ plane. The orbits are then characterized by conserved quantities \tilde{E} and \tilde{L} , the particle's energy and angular momentum per unit mass, respectively. Bound orbits are those for which $\tilde{E} < 1$ and $\tilde{L} \geq 2\sqrt{3}M$. These possess two radial turning points r_\pm ($r_- < r_+$), the periaapsis and apoapsis. Following Refs. [21, 22], these orbits can be parametrized in terms of a dimensionless semilatus rectum p and eccentricity e , such that $r_\pm = pM/(1 \mp e)$. This p - e parametrization is geometrically informative: p is a measure of the size of the orbit, while e is a measure of deviation from circularity. We note, however, that it is meaningful only for the space of bound orbits for which $\{\tilde{E} < 1, \tilde{L} > 2\sqrt{3}M\}$ is mapped onto $\{0 \leq e < 1, p \geq 6 + 2e\}$. The separatrix $p = 6 + 2e$ corresponds to unstable circular orbits and represents the boundary in p - e space separating bound from plunging orbits.

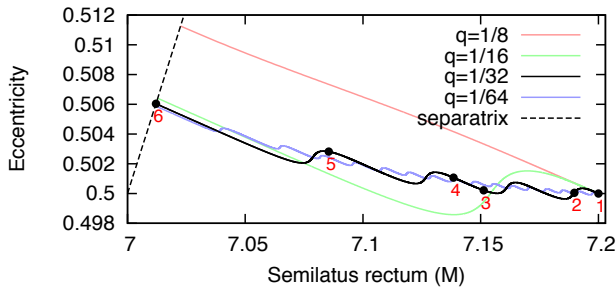


FIG. 3. (Color online) Orbital evolution in p - e space, for an orbit that begins with $p = 7.2, e = 0.5$. Each oscillation in these tracks corresponds to one full radial cycle.

In this parametrization, orbits are described by

$$r(t) = \frac{Mp}{1 + e \cos(\chi - w)} \quad (4)$$

$$\frac{d\phi}{dt} = \left[1 - \frac{2Mr'}{r-2M} \right] \times \frac{[p-2-2e \cos(\chi-w)][1+e \cos(\chi-w)]^2}{M\sqrt{p^3[(p-2)^2-4e^2]}}, \quad (5)$$

where $r \equiv r(t)$, $r'(t) \equiv \frac{dr}{dt}$, $p \equiv p(t)$, $e \equiv e(t)$, $\chi \equiv \chi(t)$ and $w \equiv w(t)$ are functions of the Kerr-Schild time coordinate t and where $\chi(t)$ monotonically increases with t . For geodesic motion, $p(t)$, $e(t)$, and $w(t)$ remain constant; they do, however, evolve under the influence of the self-force.

The orbit we consider here starts at $p_0 = 7.2, e_0 = 0.5$. In Fig. 1, we display an evolved orbit with dimensionless charge $q := \bar{q}/M = 1/32$, alongside a test-particle orbit for reference. Certain reference points along the orbit are identified to ease comparison with our other plots. As initial data, we choose $\Phi^R(t=0) = 0$ and $\dot{\Phi}^R(t=0) = 0$ and set the particle initially moving along the geodesic specified by $p_0 = 7.2, e_0 = 0.5$. This choice results in a burst of junk radiation, which contaminates the computed self-force at early times but eventually goes off the grid. By around $t = 200M$, the evolved field Φ^R settles down to give the appropriate geodesic self-force, as seen in Fig. 5. At $t = 400M$, when the particle is very close to apoapsis, the computed self-force is allowed to act on the particle, and the system of equations (1), (2), and (3) is evolved simultaneously for all subsequent times. For this particular case ($q = 1/32$), the particle makes approximately 16 revolutions (~ 4 full radial cycles) before reaching the horizon.

Self-forced orbits can also be tracked in p - e space. In Fig. 3, we observe that an oscillating and secularly increasing eccentricity accompanies the monotonic decrease in p . This secular increase is a generic feature of strong-field orbits under the influence of radiation reaction [22]. The eccentricity oscillations, on the other hand, are a new feature of self-forced orbits not seen by flux-averaged models. They are due to the intrinsic periodicity in the local self-force that goes with the (quasi)periodic motion of the particle around the black hole. Indeed, it is easy to determine that $\dot{\tilde{E}} = -a_r^{\text{SF}}$ and $\dot{\tilde{L}} = a_\phi^{\text{SF}}$. A decrease in \tilde{E} , while keeping \tilde{L} constant, leads to a decrease

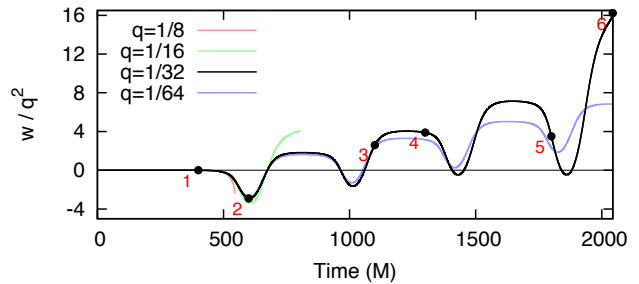


FIG. 4. (Color online) Positional element w interpreted as a measure of the periapsis shift relative to its geodesic value. The curves end when the particle crosses the separatrix.

in e , while a decrease in \tilde{L} , keeping \tilde{E} constant, tends to increase e . The self-force always decreases both \tilde{E} and $|\tilde{L}|$, but it does so at different rates depending on where the particle is. This competition between periodically varying loss rates is what leads to the oscillatory behavior in e .

Since $\dot{\tilde{E}}$ and $\dot{\tilde{L}}$ scale as q^2 , we expect that, starting from the same initial conditions, the time it takes a particle to reach the separatrix (equivalently, the number of radial cycles) should scale approximately as $1/q^2$. This is confirmed by our results. For $q = 1/8$, the particle crosses the separatrix and plunges before completing one radial cycle. For $q = 1/16, 1/32$, and $1/64$, the particle plunges after one, four, and 16 full radial cycles, respectively.

It is difficult to disentangle dissipative and conservative effects of the self-force in a self-consistent evolution, since a reference geodesic [13, 23, 24] or an explicit expression for the force [21] is not available. Nevertheless, it is clear that the p - e tracks do not fully characterize the orbital evolution. The osculating elements $\{p, e\}$ are in one-to-one correspondence with $\{\tilde{E}, \tilde{L}\}$, whose rates of change are determined only by a_r^{SF} and a_ϕ^{SF} . The r component of the self-acceleration cannot be inferred from the p - e tracks alone, and instead its effect manifests in the secular change of the positional elements [21], an example of which is w in Fig. 4. The observed changes in w are completely missed by flux-averaged approximations.

The self-acceleration and mass change along the orbit is shown in Fig. 5. Only a^r and a^ϕ are plotted here; the third component a^t is easily determined from the orthogonality condition $u_\alpha a^\alpha = 0$. Inconsistent initial data contaminate the self-force early on, but this radiates away before self-consistent evolution starts at $t = 400M$. The self-force depends most sensitively on the radial position of the particle, with its strength increasing the closer the particle is to the black hole. There is a small noticeable change in the extrema of the self-force, but it is possible that this is mainly due to the small corresponding shifts in the extremal radii of the orbit. These properties likely describe the geodesic self-force as well; it will be instructive to compare self-consistent and geodesic self-forces.

Earlier we reported an upper bound of 2% on the error in our self-force calculation. While this may appear sizable, we reiterate that this is merely an upper bound which is reached *only* for very brief portions of the orbit. Our agreement with the results of Ref. [12] is, in fact, significantly better through-

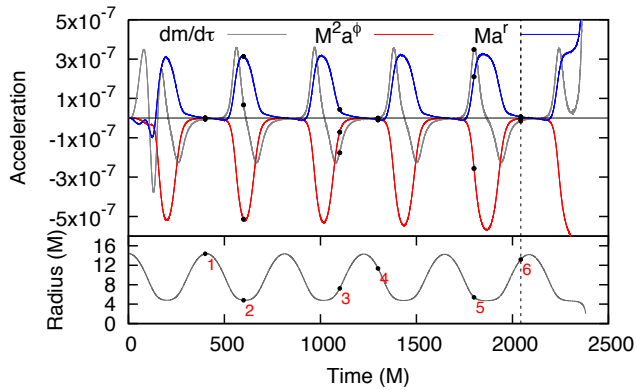


FIG. 5. (Color online) Acceleration along a trajectory that starts at $p = 7.2, e = 0.5$ for $q = 1/32$. The blue curve indicates Ma^r , the red curve $M^2 a^\phi$, and the gray curve $\frac{dm}{d\tau}$. The bottom plot shows the corresponding radial position of the particle.

out most of the orbit. By performing a higher resolution run, we found that the maximum amplitude of the error was halved. The corresponding phase at separatrix crossing, however, changed only very slightly ($\approx 0.01\%$). This suggests that the noise in the self-force does not significantly affect the phase evolution for the length of the runs we consider here.

Discussion:— We summarize by emphasizing a few points. First, our time domain 3D code is versatile: It is not limited to low eccentricities, equatorial orbits, or even the Schwarzschild spacetime. An ongoing challenge is to devise more efficient ways to evaluate the complicated expression for the effective source in the Kerr spacetime. This would, for example, allow one to check if the recently discovered Flanagan-Hinderer resonances [25] persist in a self-consistent orbit. Second, our approach makes it possible to assess the adiabatic argument on which Ref. [14] is based or, for that matter, any other proposal for the computation of self-forced orbits. Third, our code readily gives self-forced waveforms at \mathcal{S}^+ (see Fig. 2). These waveforms did not require any post-processing after the computation of the orbit; instead, both the orbit and waveform are calculated simultaneously. Finally, it is possible to generalize our approach to the more important gravitational case. But in that context, we stress that care is needed in handling delicate gauge conditions [26] and possible instabilities that may be brought forth by the nonradiative low multipoles of the metric perturbation [27]. This represents the next major phase of development for the effective source program.

As is to be expected from a 3D code, the computed self-force along an orbit is limited in accuracy compared to other methods. Further development will be required to improve on this with limited computational resources. Moreover, the code is too slow for the task of mass-producing waveforms that will sufficiently sample the entire EMRI parameter space. However, we emphasize that this is not the objective of our approach. The true value of our work lies in its ability to validate assumptions and predictions arising from all other (presumably faster) approximate methods. Our results provide the

first opportunity for these proposals to demonstrate that they indeed capture all the relevant features of self-consistent orbits and waveforms.

Acknowledgements: The authors thank Eric Poisson, Abraham Harte, Leor Barack, Sam Gralla, Luis Lehner, and Frank Löffler for helpful comments and many fruitful discussions that helped shape this work and Roland Haas for sharing numerical data for the scalar self-force. Portions of this research were conducted with high performance computational resources provided by the Louisiana Optical Network Initiative (<http://www.loni.org/>) and also used the Extreme Science and Engineering Discovery Environment, which is supported by National Science Foundation Grant No. OCI-1053575 (allocation TG-MCA02N014). Some computations were also performed on the Datura cluster at the Albert Einstein Institute.

-
- [1] F. Pretorius, Phys.Rev.Lett. **95**, 121101 (2005)M. Campanelli, C. O. Lousto, P. Marronetti, and Y. Zlochower, *ibid.* **96**, 111101 (2006)J. G. Baker, J. Centrella, D.-I. Choi, M. Koppitz, and J. van Meter, *ibid.* **96**, 111102 (2006)C. O. Lousto and Y. Zlochower, *ibid.* **106**, 041101 (2011)
 - [2] P. Amaro-Seoane, J. R. Gair, M. Freitag, M. Coleman Miller, I. Mandel, *et al.*, Class.Quant.Grav. **24**, R113 (2007)
 - [3] F. D. Ryan, Phys.Rev. **D52**, 5707 (1995)N. A. Collins and S. A. Hughes, *ibid.* **D69**, 124022 (2004)K. Glampedakis and S. Babak, Class.Quant.Grav. **23**, 4167 (2006)J. R. Gair, C. Li, and I. Mandel, Phys.Rev. **D77**, 024035 (2008)
 - [4] L. Barack and C. Cutler, Phys.Rev. **D69**, 082005 (2004)
 - [5] E. Poisson, A. Pound, and I. Vega, Living Reviews in Relativity **14**, 1 (2011), <http://www.livingreviews.org/lrr-2011-7>
 - [6] L. Barack, Class.Quant.Grav. **26**, 213001 (2009)
 - [7] B. S. DeWitt and R. W. Brehme, Annals Phys. **9**, 220 (1960)Y. Mino, M. Sasaki, and T. Tanaka, Phys.Rev. **D55**, 3457 (1997)T. C. Quinn and R. M. Wald, *ibid.* **D56**, 3381 (1997)
 - [8] A. G. Smith and C. M. Will, Phys.Rev. **D22**, 1276 (1980)A. G. Wiseman, *ibid.* **D61**, 084014 (2000)
 - [9] L. Barack and A. Ori, Phys.Rev. **D61**, 061502 (2000)
 - [10] L. Barack, Phys.Rev. **D62**, 084027 (2000)L. Barack and L. M. Burko, *ibid.* **D62**, 084040 (2000)L. Barack and C. O. Lousto, *ibid.* **D66**, 061502 (2002)L. M. Burko, Phys.Rev.Lett. **84**, 4529 (2000)L. M. Diaz-Rivera, E. Messaritaki, B. F. Whiting, and S. Detweiler, Phys.Rev. **D70**, 124018 (2004)L. Barack and N. Sago, *ibid.* **D75**, 064021 (2007)S. Detweiler, *ibid.* **D77**, 124026 (2008)N. Warburton and L. Barack, *ibid.* **D81**, 084039 (2010)**D83**, 124038 (2011)
 - [11] R. Haas and E. Poisson, Phys.Rev. **D74**, 044009 (2006)S. Detweiler, E. Messaritaki, and B. F. Whiting, **D67**, 104016 (2003)
 - [12] R. Haas, Phys.Rev. **D75**, 124011 (2007)
 - [13] L. Barack and N. Sago, Phys.Rev. **D81**, 084021 (2010)
 - [14] N. Warburton, S. Akcay, L. Barack, J. R. Gair, and N. Sago, Phys.Rev. **D85**, 061501(R) (2012)
 - [15] I. Vega and S. Detweiler, Phys.Rev. **D77**, 084008 (2008)I. Vega, P. Diener, W. Tichy, and S. Detweiler, **D80**, 084021 (2009)I. Vega, B. Wardell, and P. Diener, Class.Quant.Grav. **28**, 134010 (2011)
 - [16] L. Barack and D. A. Golbourn, Phys.Rev. **D76**, 044020 (2007)L. Barack, D. A. Golbourn, and N. Sago, **D76**, 124036 (2007)S. R. Dolan and L. Barack, **D83**, 024019 (2011)S. R. Dolan, L. Barack, and B. Wardell, **D84**, 084001 (2011)

- [17] S. Detweiler and B. F. Whiting, Phys.Rev. **D67**, 024025 (2003)
- [18] B. Wardell, I. Vega, J. Thornburg, and P. Diener, arXiv:1112.6355 (to appear in March 2012 issue of Phys.Rev.D)
- [19] T. C. Quinn, Phys.Rev. **D62**, 064029 (2000)
- [20] P. Diener, I. Vega, B. Wardell, and S. Detweiler, in preparation
- [21] A. Pound and E. Poisson, Phys.Rev. **D77**, 044013 (2008)
- [22] C. Cutler, D. Kennefick, and E. Poisson, Phys.Rev. **D50**, 3816 (1994)
- [23] Y. Mino, Phys.Rev. **D67**, 084027 (2003)
- [24] T. Hinderer and E. E. Flanagan, Phys.Rev. **D78**, 064028 (2008)
- [25] E. Flanagan and T. Hinderer, “Transient resonances in the inspirals of point particles into black holes,” (2010), arXiv:1009.4923
- [26] S. E. Gralla and R. M. Wald, Class.Quant.Grav. **25**, 205009 (2008)
- [27] S. Dolan, “Self-force calculations and m -mode regularization,” Presentation at 14th Capra Meeting, Southampton